

Autoresonant Ash Removal in Mirror Machines

Eli Gudinetsky,^{1,2} Tal Miller,^{1,3} Ilan Be'ery,³ and Ido Barth^{1,*}

¹*Racah Institute of Physics, The Hebrew University of Jerusalem, Jerusalem, 91904 Israel*

²*Department of Physics, Nuclear Research Center, Negev, PO Box 9001, Beer Sheva, Israel*

³*Rafael Plasma Laboratory, Rafael Advanced Defense Systems, POB 2250, Haifa, 3102102 Israel*

(Dated: March 8, 2024)

Magnetic confinement fusion reactors produce ash particles that must be removed for efficient operation. It is suggested to use autoresonance (a continuous phase-locking between anharmonic motion and a chirped drive) to remove the ash particles from a magnetic mirror, the simplest magnetic confinement configuration. An analogy to the driven pendulum is established via the guiding center approximation. The full 3D dynamics is simulated for α particles (the byproduct of DT fusion) in agreement with the approximated 1D model. Monte Carlo simulations sampling the phase space of initial conditions are used to quantify the efficiency of the method. The DT fuel particles are out of the bandwidth of the chirped drive and, therefore, stay in the mirror for ongoing fusion. The method is also applicable for advanced, aneutronic reactors, such as p-¹¹B.

The most straightforward magnetic confinement configuration is the magnetic mirror and thus serves as the basic building block for various linear fusion machines that are advantageous not only for their engineering simplicity but also for their high- β steady-state operation [1]. The fusion byproducts, e.g., α particles in deuterium-tritium (DT) fusion, are trapped by the same mirroring magnetic field that traps the fuel particles, taking up the place of the valuable fuel particles. The removal of the fusion ash particles poses a long-standing problem [2–10]. One of the leading methods is the α -channelling, which employs rf-waves to induce directed diffusion of the α particles while cooling down and transferring their energy through the plasma waves to the fuel particles [8, 9]. Retaining the energy of the 3.5MeV α particles in the plasma is beneficial for a self-sustaining burning process [11, 12]. However, further heating beyond ~ 15 keV could be counterproductive for DT fusion due to decreased reactivity and increased bremsstrahlung radiation losses[12]. Thus, the removal of the high-energy α particles from the fusion cell with (part of) their energy is advantageous in this scenario, particularly if the energy of the α beam can be extracted by direct energy conversion outside the mirror [13, 14]. Notably, the combination of energy-retained and energy-released α removal methods can be utilized to control the temperature in the reactor for fusion optimization.

Autoresonance (AR), i.e., a continuous phase locking in a nonlinear oscillatory system with slowly varying parameters, has been thoroughly studied theoretically [15–22] and experimentally [23–28] in various systems, where the simplest example is the chirped-driven pendulum [29]. Phase-locking is established when the driving frequency passes through the linear resonance and is preserved as the nonlinear frequency shift compensates for the chirped driving frequency. AR provides control of the oscillating degree of freedom without the need for feedback and, thus, can be used to release charged particles from a trapping potential, e.g., anti-protons from a Penning trap for anti-hydrogen production [27, 30]. The capture into resonance of the chirped-driven pendulum has two different limits. The first is the probabilistic capture, where the oscillating particle begins at a large amplitude state, and only

a small fraction of the initial oscillation phases is captured into resonance, while all other particles experience a transient resonant kick and continue in a nonresonant motion [22, 31]. The second limit is the automatic capture, where almost all particles near equilibrium are captured into AR regardless of their initial phase. The capture in this case occurs only if the driving amplitude, ε , exceeds a critical value, ε_{cr} that scales as $\alpha^{3/4}$, where α is the chirp rate [19, 20, 23]. Notably, the captured particles may reach large amplitudes as the chirping of the driving frequency continues.

In this letter, we study AR in a magnetic mirror for the first time and propose its application for fusion ash removal. The idea is to autoresonantly increase the longitudinal energy of the α particles until they escape through the loss cone. The driving force is realized via a weak oscillating axial magnetic field with a slowly down-chirped frequency that passes through the linear bouncing frequency. As a result, most of the α particles near the machine's center are phase-locked with the drive and gain axial velocity until they escape through the loss cone. Such an AR cycle can be successively repeated for continuous ash removal in a burning plasma. Crucially, the ash removal is accomplished without significantly affecting the fuel particles.

Consider a charged particle with mass m and charge q trapped in a magnetic mirror of length $2l$ and driven by a slowly chirped oscillatory field. We approximate the longitudinal magnetic field near the mirror axis in cylindrical coordinates, (r, θ, z) , as

$$B_z = B_{\min} + B_0 \left(1 - \cos \frac{\pi z}{l} \right) + \varepsilon B_0 \frac{\pi z}{l} \cos \phi_d \quad (1)$$

where $B_0 = (B_{\max} - B_{\min})/2$ and the maximum (minimum) static magnetic field is B_{\max} (B_{\min}). The last term is Eq. (1) is the time-dependent driving field, where $\varepsilon \ll 1$ is the dimensionless amplitude and $\phi_d = \int \omega_d dt$ is the phase of the chirped frequency, $\omega_d = \omega_0 - \alpha \omega_0^2 t$. The driving frequency, ω_d , is chosen such that around $t = 0$ it will resonate with the longitudinal (z -direction) bouncing frequency, $\omega_B = \sqrt{\mu B_0 \pi^2 / m l^2}$ of a typical trapped particle (see Eq. 5 below). The magnetic moment, $\mu = 0.5 m v_{\perp}^2 / B_z$ is an adiabatic invariant be-

cause $\omega_B, \omega_d \ll \omega_c$, where ω_c is the cyclotron frequency. The driving field can be realized by oscillating the currents in the mirror coils. Because of the symmetry of the mirror, the azimuthal magnetic field, B_θ is zero, while the radial component is determined by

$$B_r = -\frac{1}{2}r \frac{dB_z}{dz} \quad (2)$$

due to the magnetic Gauss' law, $\nabla \cdot \mathbf{B} = 0$. The time-varying components of the magnetic field, i.e., the driving field, induce an azimuthal electric field,

$$\mathbf{E}_d = -\frac{1}{2}r \frac{\partial B_z}{\partial t} \hat{\theta}. \quad (3)$$

Most notably, the 3D dynamics can be reduced into 1D by employing the guiding center approximation provided $mcv_0/qB_0l \ll 1$. The approximated longitudinal (along the magnetic field) equation of motion then reads [32]

$$m \frac{dv_{\parallel}}{dt} \approx qE_{\parallel} - \mu \frac{\partial B}{\partial s} + m \mathbf{u}_E \cdot \frac{d\hat{e}_1}{dt} \quad (4)$$

where we neglected gravitation. E_{\parallel} is the longitudinal components of the electric field evaluated at the guiding center trajectory. The derivative $\partial/\partial s$ is along the field line, \mathbf{u}_E is the $E \times B$ drift velocity, and \hat{e}_1 is a unit vector along the field line. For a guiding center trajectory on the mirror axis, we can thus substitute $\partial/\partial s = \partial/\partial z$ and $\hat{e}_1 = \hat{z}$. Notably, for the fields of Eqs. (1-3), the only nonvanishing term is $\mu \partial B/\partial s$ because Eq. (3) yields $E_{\parallel} = 0$ and thus also $\mathbf{u}_E(r=0) = 0$. Consequently, the guiding center equation for the longitudinal motion of particles near the mirror axis reduces to the well-studied, 1D chirped-driven pendulum [19, 20, 29]

$$\frac{dv_{\parallel}}{dt} = \frac{\mu B_0 \pi}{ml} \left(\sin \frac{\pi z}{l} + \varepsilon \cos \varphi_d \right). \quad (5)$$

Therefore, we expect to observe AR dynamics in magnetic mirrors for suitable parameters.

To test this prediction, we solve the 3D equation of motion for a nonrelativistic α particle (initial energy of 3.5 MeV) under the influence of the magnetic and electric fields in Eqs (1-3). Our solver is based on a 3D volume-preserving scheme [33] of the Lorentz force. We consider $l = 10\text{m}$, $B_{\min} = 1\text{T}$, and $B_{\max} = 3\text{T}$, which satisfies the guiding center approximation since $mcv_0/qB_0l \approx 0.01$. The initial conditions of the α particle were near equilibrium, i.e., at the mid-plane of the mirror, gyro-center on the mirror axis, and zero longitudinal velocity, so $\omega_B \approx 2\pi \times 0.9\text{ MHz}$. The driving parameters were $\omega_0 = 2\pi \times 0.8\text{ MHz}$, $\alpha = 10^{-4}$, and $\varepsilon = 2 \times 10^{-2}$, corresponding to about 60mT maximal driving magnetic field at the throat of the mirror.

The numerical results are presented in Fig. 1, exhibiting a typical AR solution (dotted red line), including the capture into resonance when passing through the linear resonance at $t \approx 0$ and the slow modulation of the energy in the weakly

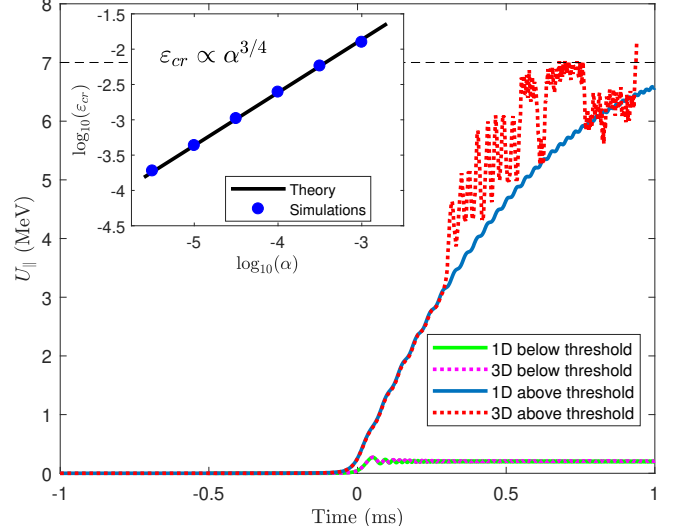


FIG. 1. The dynamics of the axial energy (evaluated at the mirror mid-plane), under the influence of the chirped drive above, $\varepsilon > \varepsilon_{\text{cr}}$, (blue and red) and below, $\varepsilon < \varepsilon_{\text{cr}}$, (green and magenta) the threshold, for the 1D guiding center approximate model (solid lines) and the 3D simulations (dotted lines). The dashed black line indicates the escape axial energy. Inset: The threshold, ε_{cr} , versus the chirp rate, α , in log-log scales, as found in 3D simulations (dots) in comparison to the theoretical scaling (solid line).

nonlinear regime [29]. The particle escapes through the loss cone at $t \approx 1\text{ms}$ when its parallel energy reaches 7MeV. We compare the full 3D solution with the 1D approximated dynamics of Eq. (5) (solid blue line) for the same parameters and found an excellent agreement until the particle is excited to higher energies (at $t \approx 0.3\text{ ms}$). The deviation from the 1D trajectory at high amplitudes is probably because of nonlinear coupling with other degrees of freedom. In the figure, we also illustrate the dynamics below the AR threshold, where the axial energy, U_{\parallel} , is modestly excited when passing through the linear resonance at $t \approx 0$ followed by energy saturation for $t > 0.1\text{ ms}$. The parameters, in this case, were the same as before except the driving amplitude, $\varepsilon = 2 \times 10^{-3}$, which was below the threshold for these parameters, $\varepsilon_{\text{cr}} \approx 2.5 \times 10^{-3}$. Since the particle energy remains relatively small, the agreement between the 3D (dotted magenta) and the approximated 1D (solid green) simulations is excellent at all times. We further study the threshold effect by scanning ε for a fixed α and finding the critical value, ε_{cr} , that separates the captured and non-captured solutions. The 3D simulations results (dots in the inset of Fig. 1) well agree with the theoretical scaling, $\varepsilon_{\text{cr}} \sim \alpha^{3/4}$, which was developed for the 1D autoresonant pendulum [18], for three orders of magnitude (solid line).

A chirp cycle from $\omega_d \approx \omega_B$ to the lower limit for the loss cone crossing, $\omega_d = 0$, lasts

$$\Delta t = \frac{\Delta\omega_d}{\alpha\omega_0^2} \approx \frac{1}{\alpha\omega_0}, \quad (6)$$

where for the above parameters $\Delta t \approx 2\text{ ms}$. This short time

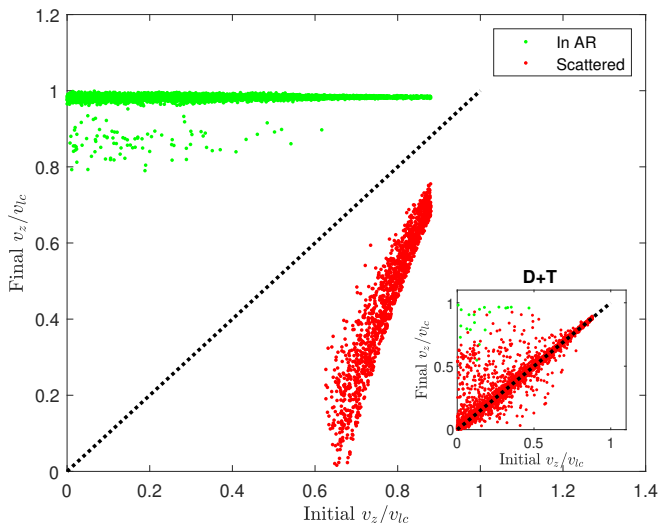


FIG. 2. Final versus initial axial velocities normalized by the loss cone velocity, v_{lc} , of autoresonant α particles (green dots) and non-captured particles (red dots). Inset: same plot for DT particles.

scale and the effect of automatic capture suggest using AR for removing α particles from mirror (fusion) machines. However, for efficient ash removal, a significant phase-space volume of initial conditions must be captured into AR, and the chirp duration must be shorter than a typical fusion burn time. To estimate the phase space efficiency of the AR ash removal, we numerically solved the 3D dynamics of 10^4 fusion ash (3.5 MeV) α particles confined in the mirror. The initial velocity directions were randomly sampled for a good phase space covering, while the system parameters were as in the example of Fig. 1. The simulation time was chosen such that the driving frequency, ω_d , begins at 1 MHz (above the linear resonance $\omega_d = \omega_B$), chirps down to 160 KHz because, practically, autoresonant particles escape before $\omega_d = 0$ due to nonlinearity and stochasticity near the separatrix.

Fig. 2 presents the change (final vs. initial) in the axial velocity, v_z , normalized by the loss cone escape velocity, $v_{lc} = 2\sqrt{\mu B_0/m}$, under the influence of the chirped drive for particles starting on the mid-plane, $z = 0$, but with different v_z . In these calculations, a particle is said to be captured into AR if its axial velocity exceeds $0.8v_{lc}$, where the last mile outward can be supported by Coulomb collisions or nonresonant stochastic kicks induced by the successive drive cycles. The figure demonstrates that all particles starting with small initial axial velocities, $v_z \leq 0.6v_{lc}$, are captured into AR as expected in the automatic capture regime. In contrast, only part of the particles with higher initial v_z are captured and can be associated with the stochastic capture regime [22, 31]. Constructively, non-captured particles (red dots) are scattered towards lower axial velocities, making them more susceptible to AR removal for the successive chirping cycle. At the same time, the DT fuel particles stay mostly unaffected by the chirped drive due to their lower mirror-bouncing frequencies as they are significantly less energetic (~ 15 keV), so only a small

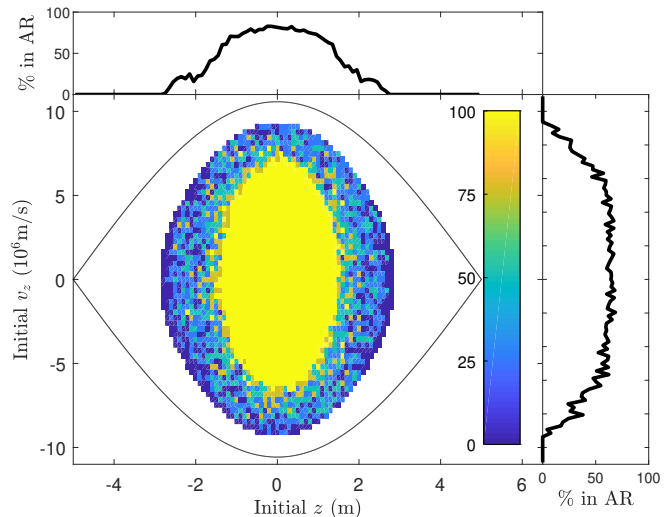


FIG. 3. Autoresonant capture probability of on-axis α particles in the $z - v_z$ initial condition phase space. The black lines denote the mirror separatrix. The outside panels display the marginal capture probability distribution in the v_z (right) and z (top) axes.

fraction of their Maxwellian distribution have a sufficiently large μ for having ω_B in the AR chirping bandwidth. This prediction is supported by the simulation results presented in the inset of Fig. 2, showing that most of the DT fuel population remains close to the no-change line (dotted), $v_{\text{final}} = v_{\text{initial}}$.

We generalize the study from mid-plane initial conditions to particles starting at the $z - v_z$ phase space but still with a gyrocenter on the mirror axis. In Fig. 3, 10^4 particles were randomly sampled and binned, where, in each bin (pixel), the capture probability was calculated as the fraction of particles captured into AR in the bin. The simulation results demonstrate the existence of automatic (the central yellow elliptic region) and stochastic (the outer ring) capture into resonance regimes. It was also found that the automatic capture phase space volume increases with ϵ (not presented).

Finally, we study how the chirped drive affects α particles starting off-axis, i.e., gyrating around $r > 0$. In the calculations presented in Fig. 4, the initial off-axis distance was tested up to 0.5 m. The simulation results (upper panel) show a weak dependency of the capture probability on the initial gyro-radius, implying the robustness of the AR control for a reasonable range of radii. It is noted that most of the α particles are born near the center (axially and radially) of a prospective fusion mirror-based machine, where the typical radial length for system parameters considered here is about 0.15 m [34, 35]. Therefore, the efficiency of a single AR ash removal cycle, which can be calculated by integrating the capture probability function (Figs. 2–3) over the initial particle distribution in $v_z - z - r$ phase space, is expected to be high.

The temporal efficiency depends on comparing the time required to accumulate an acceptable amount of α particles in the reactor and the AR removal time. We estimate the α accumulation time by $f/n_{\text{DT}}\langle\sigma v\rangle$, where f is the desired ash to

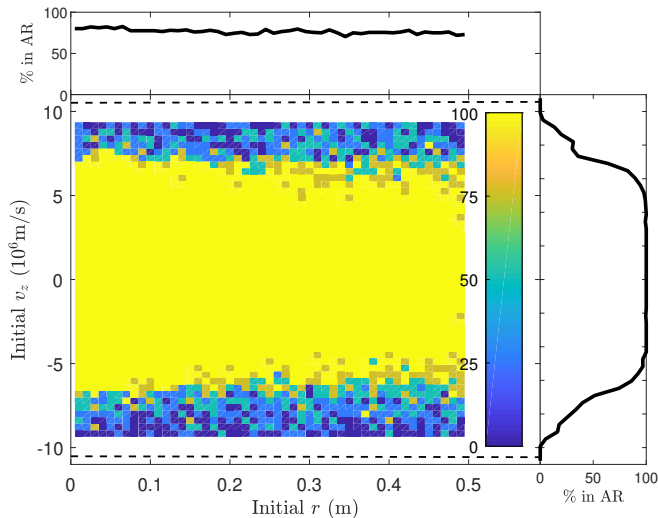


FIG. 4. AR capture probability of off-axis α particles in the $r - v_z$ initial condition phase space. The dashed black lines indicate the loss cone velocities. The outside panels display the marginal capture probability distribution in the v_z (right) and r (top) axes.

fuel particle ratio, n_{DT} is the fuel density, and $\langle\sigma v\rangle$ is averaged fusion reactivity. For example, for $f = 10^{-3}$, and plasma temperature and density of 15 keV and 10^{14} cm^{-3} , respectively, one finds a production time of ~ 25 ms, which is sufficiently longer than the 2 ms AR chirp cycle that removes most of the accumulated ash particle.

Collisions affect the capture into AR by increasing the threshold value, ε_{cr} and broadening its width [20]. These effects can be overcome for weak collisions by increasing the driving amplitude, ε . Since the typical cooling time of an α particle is hundreds of milliseconds while the chirping time is less than 2 ms, the considered system is weakly collisional.

The total energy of autoresonant particles in a magnetic mirror increases while their magnetic moment is preserved. Therefore, the energy required to autoresonantly extract a particle from the trap is $\Delta U_{AR} = (R - 1)U_{\perp} - U_{\parallel}$, where U_{\perp} and U_{\parallel} are the initial perpendicular and parallel kinetic energies, respectively, as evaluated at the mirror mid-plane, and $R = B_{max}/B_{min}$ is the mirror ratio. However, most of the energy of the removed α particles can be recovered via a direct energy conversion scheme [13, 14] where their final energy is between 3.5 MeV and RU_{\perp} . Furthermore, suppose the α particles are allowed to collisionally (or by other means) slow down until their velocity distribution settles with a mean energy of, say, 1.3 MeV [36], the energy required to remove them from the mirror reduces significantly. Yet, these slower particles can be autoresonantly targeted by tuning the driving frequency bandwidth while leaving the fast particles almost unperturbed.

We also note that while an efficient and prompt removal of α particles is essential for the continuous operation of DT reactors, it is of an absolute necessity for p- ^{11}B reactors [37] because of their low reactivity and to avoid unwanted, sec-

ondary neutronic reactions. Fortunately, the spectral separation between the α byproduct and the ^{11}B fuel particles enables utilizing AR for quick and efficient ash removal in such advanced reactors.

In conclusion, α particles born in mirror machines can be efficiently removed by an autoresonant control of their axial motion. This novel scheme is based on a 1D guiding-center theory and supported by 3D numerical simulations. Because of the spectral separation between the species' bouncing frequency bands, it is possible to extract a significant portion of the ash while leaving the fuel particles nearly unaffected. Phase space Monte Carlo analysis, including off-axis particles, verified the effectiveness and robustness of the scheme. The AR selective expulsion method is also expected to be useful for fusion fuels other than DT. It remains to study the application in more complex open-field configurations, including the field reversal configuration and the tandem machine. Future potential applications of AR in mirror systems include ash removal in aneutronic fusion, space propulsion, heavy impurities removal [38], as well as manipulating banana orbit in toroidal systems.

The authors thank Robert G. Littlejohn and Nathaniel J. Fisch for helpful conversations. This work was supported by the PAZY Foundation, Grant No. 2020-191.

* ido.barth@mail.huji.ac.il

- [1] R. F. Post, Nucl. Fusion **27**, 1579 (1987).
- [2] V. I. Khvesyuk, N. V. Shabrov, and A. N. Lyakhov, Fusion Technology **27**, 406 (1995).
- [3] N. J. Fisch, Phys. Rev. Lett. **97**, 225001 (2006).
- [4] A. J. Fetterman and N. J. Fisch, Phys. Rev. Lett. **101**, 205003 (2008).
- [5] D. Reiter, H. Keiver, G. H. Wolf, M. Baelmans, R. Behrisch, and R. Schneider, Plasma Phys. Controlled Fusion **33**, 1579 (1991).
- [6] R. White, F. Romanelli, F. Cianfrani, and E. Valeo, Phys. Plasmas **28**, 012503 (2021).
- [7] A. Bierwage, K. Shinohara, Y. O. Kazakov, V. G. Kiptily, P. Lauber, M. Nocente, Z. Stancar, S. Sumida, M. Yagi, J. Garcia, S. Ide, and JET Contributors, Nat. Commun. **13**, 3941 (2022).
- [8] N. J. Fisch, J.-M. Rax, Phys. Rev. Lett. **69**, 612 (1992).
- [9] A. I. Zhmoginov, N. J. Fisch, Phys. Plasmas **15**, 042506 (2008).
- [10] N. J. Fisch and M. C. Herrmann, Nucl. Fusion **34**, 1541(1994).
- [11] J. D. Lawson, Proc. Phys. Soc. B **70**, 6 (1957).
- [12] S. E. Wurzel, and S. C. Hsu, Phys. Plasmas **29**, 062103 (2022).
- [13] R. W. Moir and W. L. Barr, Nucl. Fusion **13**, 35 (1973).
- [14] W. L. Barr, R. W. Moir, and G. W. Hamilton, J. Fusion Energy. **2**, 131 (1982).
- [15] B. Meerson and L. Friedland, Phys. Rev. A **41**, 5233 (1990).
- [16] W. K. Liu, B. Wu, and J. M. Yuan, Phys. Rev. Lett. **75**, 1292 (1995).
- [17] L. Friedland, Phys. Rev. E **58**, 3865 (1998).
- [18] J. Fajans, and L. Friedland, **69**, 1096 (2001).
- [19] L. Friedland, J. Physics A: Mathematical And Theoretical **41**, 415101 (2008).
- [20] I. Barth, L. Friedland, E. Sarid, and A. G. Shagalov, Phys. Rev. Lett. **103**, 155001 (2009).
- [21] I. Barth and L. Friedland, Phys. Rev. Lett. **113**, 040403 (2014).

- [22] T. Armon and L. Friedland, *J. Plasma Phys.* **82**, 705820501 (2016).
- [23] J. Fajans, E. Gilson, and L. Friedland, *Phys. Rev. Lett.* **82**, 4444 (1999).
- [24] O. Naaman, J. Aumentado, L. Friedland, J. S. Wurtele, and I. Siddiqi, *Phys. Rev. Lett.* **101**, 117005 (2008).
- [25] A. Barak, Y. Lamhot, L. Friedland, and M. Segev, *Phys. Rev. Lett.* **103**, 123901 (2009).
- [26] K. W. Murch, R. Vijay, I. Barth, O. Naaman, J. Aumentado, L. Friedland, and I. Siddiqi, *Nat. Phys.* **7**, 105 (2011).
- [27] G. B. Andresen *et al.* (ALPHA Collaboration), *Phys. Rev. Lett.* **106**, 025002 (2011).
- [28] Y. Shalibo, Y. Rofe, I. Barth, L. Friedland, R. Bialczack, J. M. Martinis, and N. Katz, *Phys. Rev. Lett.* **108**, 037701 (2012).
- [29] L. Friedland, in *Proceedings. 2005 International Conference Physics And Control.* (2005) pp. 8-14.
- [30] G. B. Andresen *et al.* (ALPHA Collaboration), *Nature* **468** 673 (2010).
- [31] A. Neishtadt and A. Vasiliev, *Phys. Rev. E* **71**, 056623 (2005).
- [32] T. G. Northrop, *The Adiabatic Motion Of Charged Particles* (Interscience Publishers, New York, 1963) p. 9.
- [33] Y. He, Y. Sun, J. Liu, and H. Qin, *J. Comput. Phys.* **281** 135 (2015).
- [34] P. A. Bagryansky, A. V. Anikeev, G. G. Denisov, E. D. Gospodchikov, A. A. Ivanov, A. A. Lizunov, Yu. V. Kovalenko, V. I. Malygin, V. V. Maximov, O. A. Korobeinikova, S. V. Murakhtin, E. I. Pinzhenin, V. V. Prikhodko, V. Ya. Savkin, A. G. Shalashov, O. B. Smolyakova, E. I. Soldatkina, A. L. Solomakhin, D. V. Yakovlev, and K. V. Zaytsev, *Nucl. Fusion* **55**, 053009 (2015).
- [35] P. A. Bagryansky, A. G. Shalashov, E. D. Gospodchikov, A. A. Lizunov, V. V. Maximov, V. V. Prikhodko, E. I. Soldatkina, A. L. Solomakhin, and D. V. Yakovlev, *Phys. Rev. Lett.* **114**, 205001 (2015).
- [36] W. W. Heidbrink and G. J. Sadler, *Nucl. Fusion* **34**, 535 (1994).
- [37] E. J. Kolmes, I. E. Ochs, and N. J. Fisch, *Phys. Plasmas* **29**, 110701 (2022).
- [38] E. J. Kolmes, I. E. Ochs, and N. J. Fisch, *Phys. Plasmas* **25**, 032508 (2018).